PCCP

PAPER

View Article Online
View Journal | View Issue

Cite this: *Phys. Chem. Chem. Phys.*, 2014, **16**, 4962

Study by electrical conductivity measurements of semiconductive and redox properties of M-doped NiO (M = Li, Mg, Al, Ga, Ti, Nb) catalysts for the oxidative dehydrogenation of ethane

Ionel Popescu,[a] Eleni Heracleous,[b] Zinovia Skoufa,[c] Angeliki Lemonidou[bc] and Ioan-Cezar Marcu*[ad]

Received 14th November 2013,
Accepted 3rd January 2014

DOI: 10.1039/c3cp54817a

www.rsc.org/pccp

Pure and M-doped nickel oxides with M = Li, Mg, Al, Ga, Ti, Nb, catalysts for the oxidative dehydrogenation of ethane into ethylene, were characterized by *in situ* electrical conductivity measurements. Their electrical conductivity was studied as a function of temperature and oxygen partial pressure and was followed with time during sequential exposures to air, an ethane–air mixture (reaction mixture) and pure ethane under conditions similar to those of catalysis. All the materials appeared to be p-type semiconductors under air with positive holes as the main charge carriers and their electrical conductivity decreased in the following order: Li–NiO > NiO > Mg–NiO > Nb–NiO > Ga–NiO > Al–NiO > Ti–NiO. All the catalysts remained p-type semiconductors in the reaction mixture at 400 °C. Correlations between the p-type semiconductivity and the catalytic properties have been evidenced. The reaction mechanism involves surface lattice O^- species and can be assimilated to a Mars and van Krevelen mechanism.

1. Introduction

It is well known that the electronic and redox properties of oxide-based catalysts strongly influence their catalytic performance in both selective and total oxidation reactions.[1] This is why, establishing relationships between the electronic and redox properties of oxide catalysts and their activity and/or selectivity is essential for a better understanding of the reaction mechanism and, consequently, for improving their catalytic performances on a scientific basis or for a rational design of new efficient catalysts. A useful technique to characterize the electronic and redox properties of oxidation catalysts is the electrical conductivity measurement,[2] a high number of papers being dedicated in the last decade to this subject.[3–14] Numerous previous studies have correlated the conductivity of the oxide materials with their catalytic performance in partial oxidation reactions like, for example, ethane to ethene,[15,16] propane to propene,[17–19] *n*-butane to butenes[4,20] and *n*-butane to maleic anhydride.[21,22] Investigation of $La_{1-x}Sr_xFeO_{3-\delta}$ perovskites and Mn-based oxides demonstrated the importance of p-type semiconductivity for catalytic activity in ethane ODH, similar to what has been determined for the oxidative coupling of methane.[15,16,23] However, p-type semiconductivity has also been related to decreased selectivity in ODH reactions. Simon and Kondratenko[11] studied the electrical and catalytic properties of materials with $Cs_x(Mo,Nb)_5O_{14}$ composition in ethane ODH and reported that secondary (non-selective) oxidation reactions are inhibited progressively with rising contributions of the n-type conductivity in the materials. The *in situ* characterization of the three pure reference phases of the V–Mg–O system (*meta*-$Mg_2V_2O_6$, *pyro*-$Mg_2V_2O_7$ and *ortho*-$Mg_3V_2O_8$) by electrical conductivity measurements explained the higher reactivity of *pyro*-$Mg_2V_2O_7$ in propane ODH, as it was the phase with the most numerous labile surface anions.[24] Marcu *et al.*[4] were able to elucidate the differences in the catalytic reaction mechanism of Ti and Zr pyrophosphate catalysts in the oxidative dehydrogenation of *n*-butane based on the differences in the conductivity of the materials when exposed to air and *n*-butane.

Doped nickel oxide has recently been reported as an efficient catalyst for the low temperature oxidative dehydrogenation of ethane,[25] which is an attractive alternative to the conventional steam cracking route for the production of ethylene. It is well known that NiO is a p-type semiconducting oxide being

[a] *Research Center for Catalysts and Catalytic Processes, Faculty of Chemistry, University of Bucharest, 4-12, Blv. Regina Elisabeta, 030018 Bucharest, Romania. E-mail: ioancezar.marcu@g.unibuc.ro, ioancezar_marcu@yahoo.com; Fax: +40 213159249; Tel: +40 214103178x138*
[b] *Chemical Process Engineering Research Institute (CPERI), Centre for Research and Technology Hellas (CERTH), 6th km Charilaou – Thermi Road, P.O. Box 361, 57001 Thessaloniki, Greece*
[c] *Department of Chemical Engineering, Aristotle University of Thessaloniki, University Campus, 54124 Thessaloniki, Greece*
[d] *Laboratory of Chemical Technology and Catalysis, Department of Organic Chemistry, Biochemistry and Catalysis, Faculty of Chemistry, University of Bucharest, 4-12, Blv. Regina Elisabeta, 030018 Bucharest, Romania*

characterized by an excess of lattice oxygen anions associated with the existence of positive holes as main charge carriers.[2] The electrical conductivity and, thus, the concentration of positive holes can be controlled by doping NiO with controlled amounts of heterovalent cationic species with compatible ion sizes.[2] If the doping cation valence is larger than that of the host cation, *i.e.* Ni^{2+}, a decrease of the electrical conductivity and thus of the concentration of positive holes is expected. Inversely, if the doping cation valence is smaller than that of the host cation, an increase of the electrical conductivity and thus of the concentration of positive holes is expected.

Oxidation or reduction of semiconducting oxide-based catalysts can be evidenced by following the evolution of their electrical conductivity as a function of the nature of the gas phase in contact with the solid. Thus, exposure of a p-type oxide to oxygen leads to the increase of its electrical conductivity with respect to that in an inert atmosphere, according to the following equilibrium equation:

$$O_{2(gas)} \rightleftharpoons O^-_{2(ads)} + h^\bullet \rightleftharpoons 2O^-_{(ads)} + h^\bullet \rightleftharpoons 2O^{2-}_{(ads)} + 2h^\bullet \rightleftharpoons O^\times_O \quad (1)$$

where $h^\bullet$ represents a positive hole and $O^\times_O$ a lattice oxygen anion of the solid. The electrons trapped by the adsorbed oxygen are provided by the valence band of the oxide where new positive holes are created. In contrast, exposure to a reducing gas such as ethane leads to the consumption of lattice oxygen with the formation of oxygen vacancies. In this case electrons are released in the valence band of the oxide resulting in the decrease of the concentration of positive holes and thus in the decrease of the electrical conductivity.

All of the above highlight that *in situ* conductivity measurements are a powerful tool for the investigation of redox catalysts and can help elucidate the origin of differences in the catalytic behavior of selective oxidation catalysts. In this paper DC-electrical conductivity of M-doped NiO catalysts (M = Li, Mg, Al, Ga, Ti, Nb) – highly promising materials for ethane ODH – was studied as a function of the temperature, the oxygen partial pressure and the nature of different gaseous reactant atmospheres including the reaction mixture at the reaction temperature. To the best of our knowledge, such measurements on this type of materials have not been reported in the literature before. Comparisons between the different M–NiO catalysts and correlations between their semiconductive properties and their catalytic performance in the oxidative dehydrogenation of ethane into ethylene have been established.

2. Experimental

2.1. Catalysts' preparation and characterization

A series of M-doped nickel oxides, where M = Li, Mg, Al, Ga, Ti and Nb, with a M/Ni atomic ratio of 0.176 was prepared by the evaporation method, as described elsewhere.[25,26] Solutions containing both M and Ni cations were heated at 70 °C under continuous stirring for 1 h. The solvent was then removed by evaporation under reduced pressure, and the resulting solids were dried overnight at 120 °C and calcined in synthetic air at 450 °C for 5 h. Aqueous solutions of nickel nitrate and the respective metal nitrates in appropriate amounts were used for Li, Mg, Al and Ga–NiO samples. For the Ti–NiO sample a solution of nickel(II) acetate and titanium(IV) isopropoxide in ethanol was used, while for the Nb–NiO sample, an aqueous solution containing nickel nitrate and ammonium niobium oxalate was prepared. Pure NiO was obtained from the decomposition of nickel nitrate hexahydrate at 450 °C for 5 h in synthetic air.

The crystal structure of the prepared samples was controlled by X-ray diffraction. All the solids showed a well crystallized NiO-like phase. Minor amounts of TiO_2 anatase phase and an amorphous niobium-rich phase were also evidenced for Ti–NiO and Nb–NiO samples, respectively.[25]

2.2. Catalytic test

The catalytic oxidative dehydrogenation of ethane was performed in a fixed bed quartz reactor operating at atmospheric pressure, in the temperature range from 300 to 425 °C, as described elsewhere.[25] The composition of the reaction mixture used was 9.1% C_2H_6/9.1% O_2/81.8% He and the W/F ratio was varied from 0.02 to 0.71 g s cm^{-3}. The reaction products were analyzed by gas chromatography, the major products observed being ethylene and CO_2.

2.3. Electrical conductivity measurements

The oxide samples mixed with an aqueous solution of 5 wt% of polyvinyl alcohol were compressed at *ca.* 2.76×10^7 Pa using a Carver 4350.L pellet press to ensure good electrical contacts between the catalyst grains. The obtained pellet was calcined for 30 min under air at 430 °C for removing the polyvinyl alcohol binder and then placed in a horizontal quartz tube between two platinum electrodes. Flow rates of gases flowing over the sample were controlled by fine needle valves and were measured by capillary flow meters. The temperature was controlled using thermocouples soldered to the electrodes and, when short-circuited, they were used to determine the electrical conductivity σ of the samples, which can be expressed by the formula:

$$\sigma = \frac{1}{R} \times \frac{t}{S} \quad (2)$$

where R is the electrical resistance and t/S is the geometrical factor of the pellet including the thickness t (*ca.* 3 mm) and the cross sectional area S of the pellet whose diameter was equal to 13 mm. The electrical resistance was measured using a megaohmmeter (FLUKE 177 Digital Multimeter).

To compare the electrical conductivities of the samples, it is required that the solids have similar textures and surface states. Indeed, the electrical conductivity of semiconducting oxide powders can be written as:

$$\sigma = An \quad (3)$$

where n is the concentration of the main charge carriers and A is a coefficient of proportionality which includes the mobility of the main charge carriers and the elementary charge of the electron and depends on the compression of the powder and on

the number and quality of contact points between particles.[2] Since the samples were compressed at the same pressure and the electrical conductivity measurements were standardized, A can be considered similar for all the samples under identical conditions.

The common reference states for σ determination have been chosen under air at atmospheric pressure at 320 °C and at 400 °C. At these temperatures, which are in the range used in the catalytic reactions, most of the ionically adsorbed species such as H_3O^+, HO^- which would produce an additional surface conductivity are eliminated. The solid was initially heated from room temperature to the desired temperature at a heating rate of 5 °C min^{-1}.

3. Results and discussion

3.1. Catalytic performance

Although the present work is devoted to the electrical and redox properties of M-doped NiO catalysts, where M = Li, Mg, Al, Ga, Ti and Nb, it is important to mention their catalytic performance in the oxidative dehydrogenation of ethane into ethylene which was discussed in detail in ref. 25. Thus, Table 1 summarizes the main catalytic results from the testing of the samples in the oxidative dehydrogenation reaction at 400 °C. It can be observed that, except for Nb–NiO catalysts which showed the highest ethane conversion, the activity of the M–NiO catalysts roughly decreased with increasing valence of the dopant cation. This trend is further confirmed by the specific surface activity of the samples, *i.e.* the rate of ethane consumption per surface area unit. Ethylene selectivity, on the other hand, demonstrates a continuous increasing tendency with increasing valence of the dopant, indicating a gradual elimination of unselective catalytic sites leading to total oxidation reactions. Nb–NiO presents the highest selectivity towards ethylene.

3.2. Variations of the electrical conductivity as a function of temperature

The semilog plots of σ variation as a function of the temperature under air during temperature-programmed heating of the catalysts are presented in Fig. 1. It can be observed that the electrical conductivity of the samples increased regularly with the temperature, reaching a plateau for temperatures higher than 250–350 °C. This suggests that at high temperatures all the acceptor levels of the oxides are ionized, the maximum concentration of charge carriers being reached. Fig. 2 shows the variations of lg σ *versus* reciprocal temperature under air in the domain of the regular increase of electrical conductivity. The linear variations observed show that all the materials behave as semiconductors with the electrical conductivities varying exponentially with temperature according to the typical activation law:

$$\sigma = \sigma_0 \cdot \exp\left(-\frac{E_c}{RT}\right) \quad (4)$$

Table 1 Catalytic reaction data of the M-doped NiO catalysts in the oxidative dehydrogenation of ethane at 400 °C (reaction conditions: W/F = 0.54 g s cm^{-3}, C_2H_6/O_2 = 1/1)[25]

Catalyst	Dopant valence	Ethane conversion (%)	Reaction rate (μmol m^{-2} s^{-1})	Selectivity at 10% isoconversion (%)
NiO	—	28.0	0.126	20.0
Li–NiO	1	35.7	0.319	17.9
Mg–NiO	2	41.0	0.139	30.0
Al–NiO	3	25.7	0.025	63.0
Ga–NiO	3	31.9	0.047	53.0
Ti–NiO	4	14.3	0.056	77.8
Nb–NiO	5	65.6	0.058	88.3

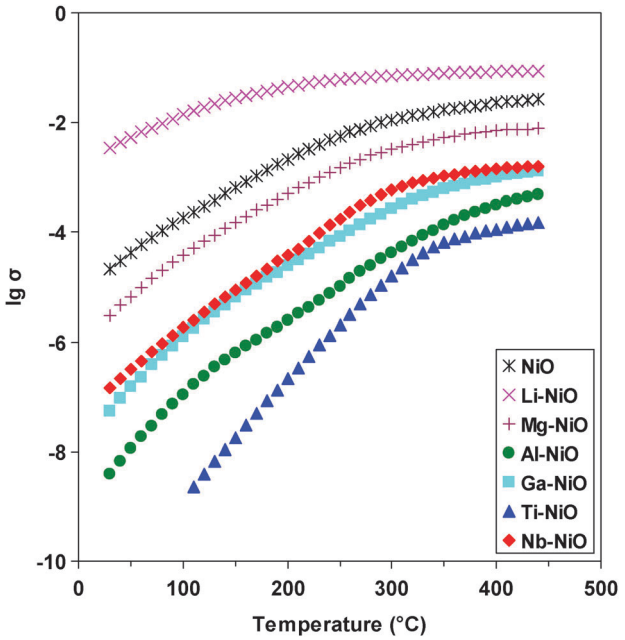

Fig. 1 Semilog plot of σ variation as a function of the temperature during temperature-programmed heating of NiO and M–NiO catalysts with M = Li, Mg, Al, Ga, Ti and Nb, under air (heating rate 5 °C min^{-1}; σ in ohm^{-1} cm^{-1}).

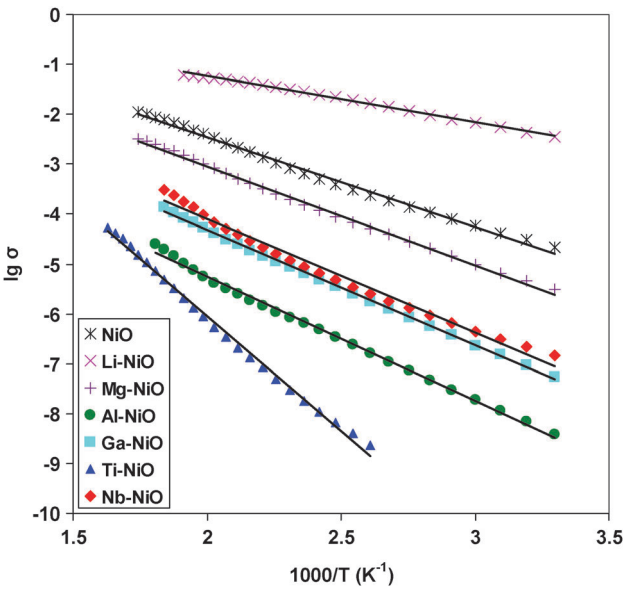

Fig. 2 Arrhenius plots for the electrical conductivity σ of NiO and M–NiO catalysts with M = Li, Mg, Al, Ga, Ti and Nb, under air (σ in ohm^{-1} cm^{-1}).

Table 2 Electrical characteristics of the M-doped NiO samples

Catalyst	E_c[a] (kJ mol^{-1})	Exponent p[b]	σ_2 (ohm^{-1} cm^{-1})
NiO	34.8	77.2[c]	1.5×10^{-4} [c]
Li–NiO	17.7	83.3[c]	1.1×10^{-2} [c]
Mg–NiO	38.2	82.6	3.7×10^{-3}
Al–NiO	48.0	22.2	4.9×10^{-5}
Ga–NiO	44.7	19.4	2.6×10^{-4}
Ti–NiO	88.5	8.3	7.8×10^{-6}
Nb–NiO	44.4	16.9	4.8×10^{-4}

[a] Activation energy of conduction. [b] From eqn (5). [c] Measurements at 100 °C.

where σ_0 is the preexponential factor and E_c is the dynamic activation energy of conduction.

The data in Fig. 2 also show that the electrical conductivity and, according to eqn (3), the concentration of the charge carriers in the solids decreased in the following order: Li–NiO > NiO > Mg–NiO > Nb–NiO > Ga–NiO > Al–NiO > Ti–NiO.

The slopes of the semi-log plots enabled the calculation of the E_c values presented in Table 2. It can be observed that the activation energy of conduction is lower for the Li–NiO sample compared to NiO reference, while it is higher for the NiO samples doped with higher valence cations, as already observed for pure and doped nickel oxides.[27] Except for the Nb–NiO sample, the activation energy of conduction increased with increasing valence of the doping cation in the following order: Li–NiO < NiO < Mg–NiO < Nb–NiO ≈ Ga–NiO < Al–NiO ≪ Ti–NiO. The observed differentiation in the Nb–NiO sample will be discussed and explained in the following paragraphs. The much higher value of the activation energy of conduction observed for the Ti–NiO sample could be explained by an electron transfer from TiO_2 to NiO, as TiO_2, detected by XRD in this sample,[25] is known to be a n-type semiconductor. This transfer is physically based on the alignment of the Fermi levels of TiO_2 and NiO.[28] Nevertheless, the quantity of TiO_2 present in the Ti–NiO sample is lower than the percolation threshold and the solid's behavior is determined by the NiO phase, *i.e.* it behaves as a p-type semiconductor (see below).

3.3. Variations of the electrical conductivity under air as a function of oxygen partial pressure

Fig. 3a shows the variations of σ as a function of oxygen pressure at 320 °C in a log–log plot. It appears that Mg–, Al–, Ga–, Ti– and Nb–NiO samples are of the p-type under oxygen since $\partial\sigma/\partial P_{O_2} > 0$, while no dependence of σ on the oxygen pressure was observed for NiO and Li–NiO samples at this temperature. As discussed above, both NiO and Li–NiO exhibit high electrical conductivity and low activation energy of conduction. Thus, the maximum concentration of charge carriers seems to be already reached at 320 °C (Fig. 1) and therefore no further changes are induced by the variation of the oxygen pressure. Indeed, this was confirmed by performing electrical conductivity measurements as a function of oxygen pressure at 100 °C over these two materials. The results, shown in Fig. 3b, demonstrate that the conductivity increases with the oxygen

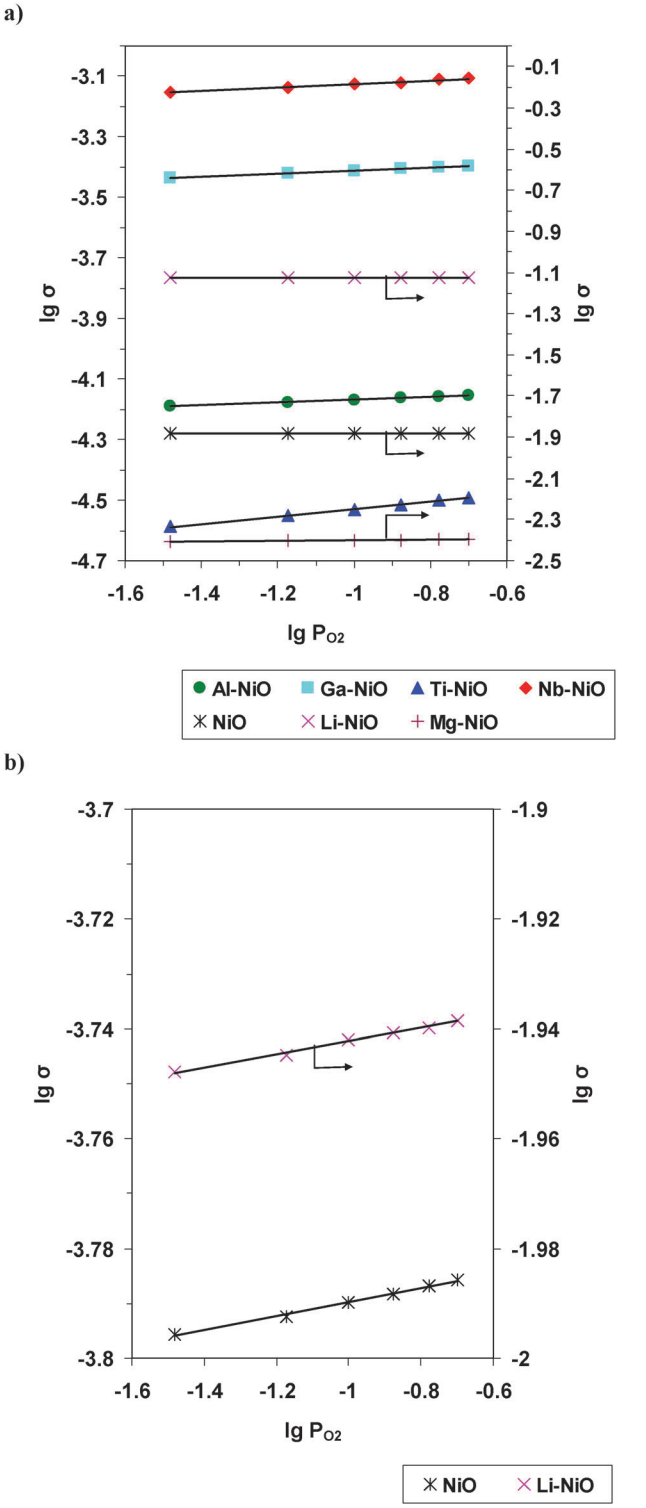

Fig. 3 Variation of σ as a function of the oxygen pressure for NiO and M–NiO catalysts with M = Li, Mg, Al, Ga, Ti and Nb, at 320 °C (a) and 100 °C (b) in a log–log plot (P_{O_2} in atm; σ in ohm^{-1} cm^{-1}).

partial pressure at 100 °C and, therefore, confirm their p-type character.

It is generally assumed that the electrical conductivity σ of p-type oxides varies as a function of partial pressure of oxygen

P_{O_2} and temperature T, according to the equation:

$$\sigma(P_{O_2}, T) = C \cdot P_{O_2}^{+1/p} \cdot \exp\left(-\frac{\Delta H_c}{RT}\right) \quad (5)$$

where ΔH_c represents the enthalpy of conduction and C is a constant which only depends on various characteristics of the sample (charge and mobility of the charge carriers, the number of contact points between grains *etc.*).[2] The value of the exponent p can be indicative of the nature of the defects in the solid, which generate charge carriers. The values of the exponent p calculated for the different solids from the slopes of the log–log plots in Fig. 3 are presented in Table 2. It can be observed that for all the samples, the value of p was significantly higher than 4 or 6 that, respectively, corresponds to the existence of singly and doubly ionized cationic vacancies. Such a phenomenon could be explained by a complex model involving two different sources of positive holes, one of them being independent of the partial pressure of oxygen:

$$\sigma = \sigma_1 + \sigma_2 \quad (6)$$

with $\sigma_1 \propto P_{O_2}^{+1/4}$ or $\sigma_1 \propto P_{O_2}^{+1/6}$ and σ_2 independent of the partial pressure of oxygen P_{O_2}. A linear relationship was obtained when plotting the total conductivity σ as a function of $P_{O_2}^{+1/6}$ for all the samples (Fig. 4). This confirmed the existence of a source of positive holes whose nature was independent of oxygen pressure in all cases. It can be associated with the substitution defects formed in the solid by doping and, in the case of NiO, with the existence of $Ni_{Ni}^{\bullet}$ substitution defects. The *y*-intercept represents the conductivity σ_2 at the temperature concerned (Table 2) and renders therefore possible the separation of the two contributions. With σ_2 known, σ_1 was calculated by subtracting σ_2 from σ according to eqn (6) and was represented as a function of the oxygen pressure in a log–log plot (Fig. 5). The obtained plots exhibit the expected +1/6 slope for all the solids in line with the model proposed. This means that the cationic vacancies present in all the considered solids are doubly ionized in agreement with the fact that all the acceptor levels of these oxides are ionized at relatively low temperature as suggested by the results presented in Fig. 1.

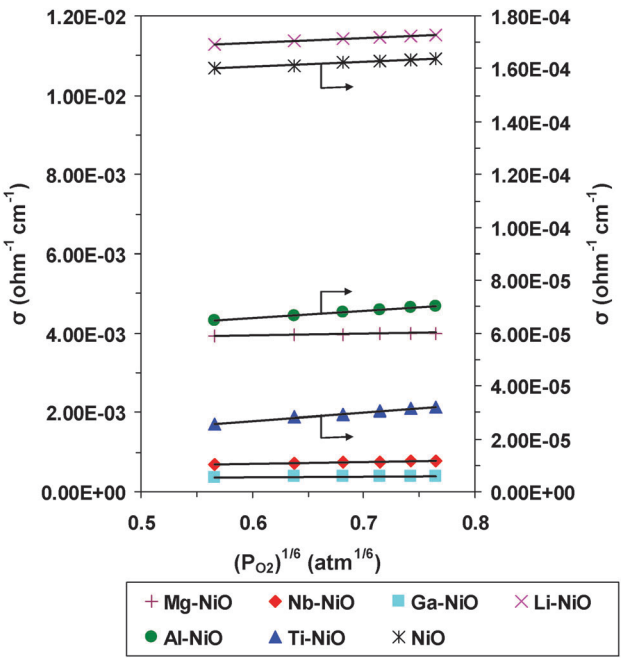

Fig. 4 Total conductivity σ *versus* $P_{O_2}^{+1/6}$ for the M–NiO catalysts, with M = Mg, Al, Ga, Ti and Nb, at 320 °C and for NiO and Li–NiO at 100 °C.

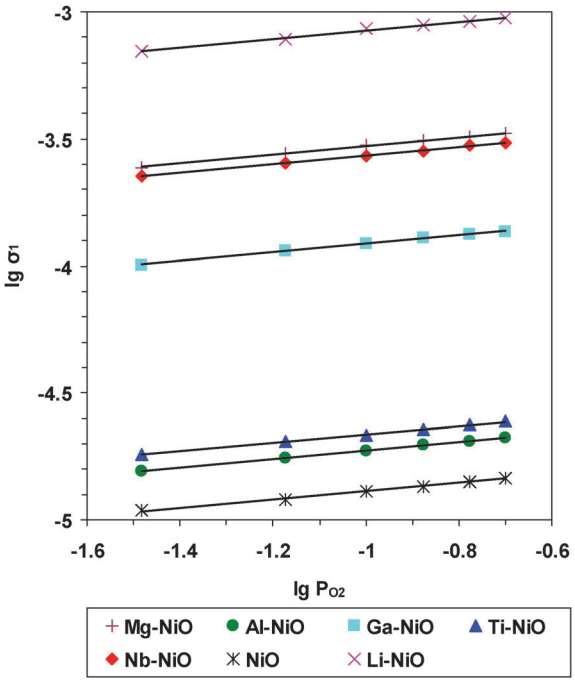

Fig. 5 Variation of σ_1 as a function of the oxygen pressure for the M–NiO catalysts, with M = Mg, Al, Ga, Ti and Nb, at 320 °C and for NiO and Li–NiO at 100 °C in a log–log plot (P_{O_2} in atm; σ_1 in ohm^{-1} cm^{-1}).

It is well known[2] that upon doping NiO with Li, the electrical conductivity increases as the charge carriers' concentration increases according to the following equation written in Kröger–Vink notation:

$$Li_2O + \tfrac{1}{2}O_2 \xrightarrow{NiO} 2Li'_{Ni} + 2O_O^{\times} + 2h^{\bullet} \quad (7)$$

where Li'_{Ni} denotes a substitutional defect of Li^+ sitting on a Ni^{2+} lattice site, $O_O^{\times}$ an oxygen anion of the solid in regular lattice points and $h^{\bullet}$ a positive hole.

The introduction of higher valence cations into NiO creates substitution defects associated with the source of positive holes whose nature is independent of oxygen pressure and decreases the concentration of charge carriers compared with NiO according to the following equations:

$$M_2O_3 + 2h^{\bullet} \xrightarrow{NiO} 2M_{Ni}^{\bullet} + 2O_O^{\times} + \tfrac{1}{2}O_2 \quad (8)$$

$$TiO_2 + 2h^{\bullet} \xrightarrow{NiO} Ti_{Ni}^{\bullet\bullet} + O_O^{\times} + \tfrac{1}{2}O_2 \quad (9)$$

$$Nb_2O_5 + 6h^{\bullet} \xrightarrow{NiO} 2Nb_{Ni}^{\bullet\bullet\bullet} + 2O_O^{\times} + \tfrac{3}{2}O_2 \quad (10)$$

or, if Nb^{5+} changes its valence to Nb^{4+}:

$$NbO_2 + 2h^{\bullet} \xrightarrow{NiO} Nb_{Ni}^{\bullet\bullet} + O_O^{\times} + \tfrac{1}{2}O_2 \quad (11)$$

where M = Al, Ga and $M^{\bullet}_{Ni}$, $Ti^{\bullet\bullet}_{Ni}$, $Nb^{\bullet\bullet\bullet}_{Ni}$, and $Nb^{\bullet\bullet}_{Ni}$ denote substitutional defects of M^{3+}, Ti^{4+}, Nb^{5+} and Nb^{4+}, respectively, sitting on Ni^{2+} lattice sites.

The doping reactions may also involve the consumption of cationic vacancies from the host NiO, as follows:

$$MgO + V''_{Ni} + 2h^{\bullet} \xrightarrow{NiO} Mg^{\times}_{Ni} + \tfrac{1}{2}O_2 \quad (12)$$

$$M_2O_3 + 2V''_{Ni} + 6h^{\bullet} \xrightarrow{NiO} 2M^{\bullet}_{Ni} + \tfrac{3}{2}O_2 \quad (M = Al \text{ and } Ga) \quad (13)$$

$$TiO_2 + V''_{Ni} + 4h^{\bullet} \xrightarrow{NiO} Ti^{\bullet\bullet}_{Ni} + O_2 \quad (14)$$

$$Nb_2O_5 + 2V''_{Ni} + 10h^{\bullet} \xrightarrow{NiO} 2Nb^{\bullet\bullet\bullet}_{Ni} + \tfrac{5}{2}O_2 \quad (15)$$

where V''_{Ni} denotes a doubly ionized nickel vacancy and $Mg^{\times}_{Ni}$ a substitutional defect of Mg^{2+} sitting on a Ni^{2+} lattice site. It is noteworthy that eqn (12) is obviously responsible for the observed decrease of the charge carriers' concentration in the case of a Mg–NiO sample compared to pure NiO although the two elements have the same valence.

As the number of moles of charge carriers (positive holes) consumed by doping increases with the doping cation valence, according to the equations above, the electrical conductivity of the samples is expected to decrease in the following order: Li–NiO > NiO > Mg–NiO > M–NiO > Ti–NiO > Nb–NiO. However, the observed order was: Li–NiO > NiO > Mg–NiO > Nb–NiO > M–NiO > Ti–NiO. This shows that the Nb–NiO sample has an electrical conductivity higher than expected based on eqn (10), (11) and (15) suggesting that the valence of doping Nb cations in the Nb–NiO sample must be lower than 5 or 4. Taking into consideration that NbO is a stable oxide having a sodium chloride type structure, just like NiO, except that 25% of the NaCl lattice sites are unoccupied,[29] we consider that it is possible that niobium is, at least partially, divalent in the Nb–NiO sample.

3.4. *In situ* electrical conductivity measurements under catalytic conditions

To get information about the solids under conditions as close as possible to those of catalysis, the electrical conductivity measurements were performed at a temperature within the reaction temperature range during sequential periods under air, in an ethane–air mixture (reaction mixture with an oxygen-to-ethane molar ratio equal to 1) and in pure ethane. The results obtained at 400 °C are displayed in Fig. 6. The solids were heated from room temperature to 400 °C, at a heating rate of 5 °C min^{-1} in air flow at atmospheric pressure. After reaching the steady state under the air flow, an ethane–air mixture (reaction mixture) was passed over the samples. For all the catalysts the electrical conductivity decreased compared to that in air, to a different extent depending on the doping cation. This behavior corresponds to the p-type semiconductive character, since, for oxide semiconductors, the p-type criterion is $\partial\sigma/\partial P_{O_2} > 0$ or, considering ethane as a reductant, $\partial\sigma/\partial P_{C_2H_6} < 0$. When air

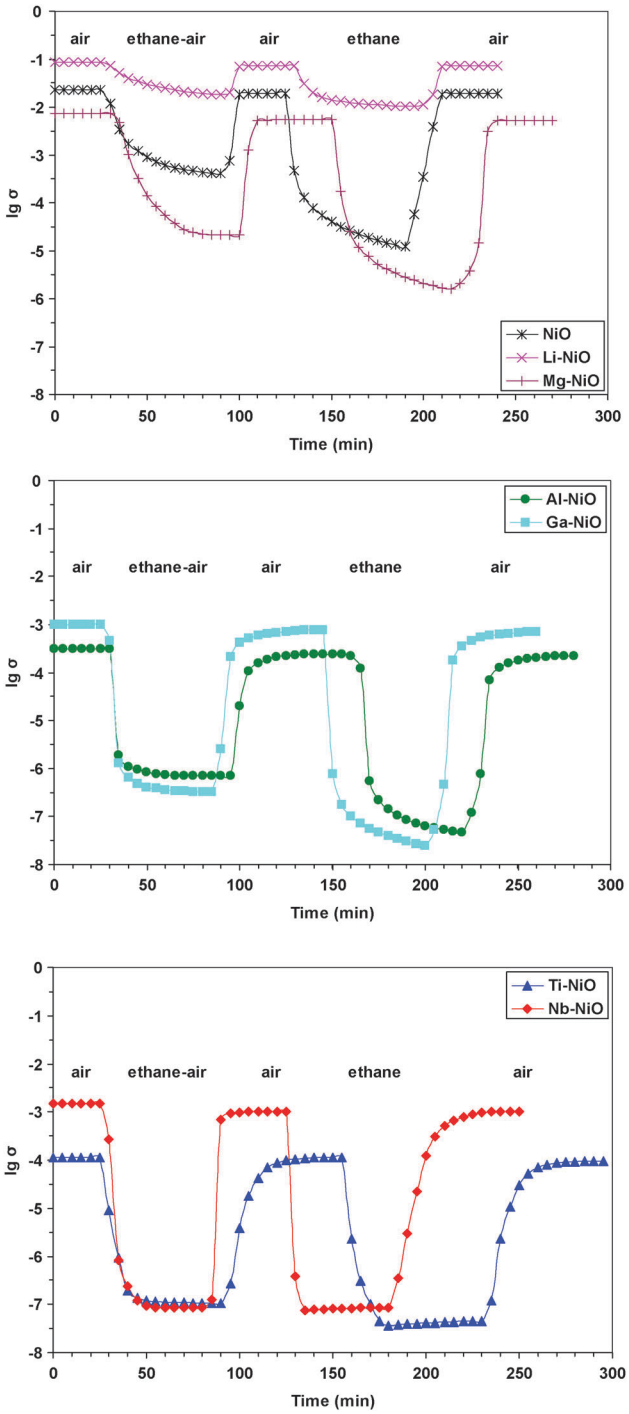

Fig. 6 Variation of the electrical conductivity during sequential exposures to air, an ethane–air mixture (reaction mixture with an oxygen-to-ethane molar ratio equal to 1) and pure ethane for NiO and M–NiO catalysts, with M = Li, Mg, Al, Ga, Ti and Nb, at 400 °C (σ in ohm^{-1} cm^{-1}).

was introduced again over the samples, the electrical conductivity increased immediately and reached a plateau corresponding to a σ value identical to the initial value suggesting that the reoxidation of the reduced solid was totally reversible. After reaching again the steady state under air flow, a sequence of pure ethane was introduced over the samples. The electrical conductivity

strongly decreased reaching a plateau corresponding to the steady state of the reduced solid in pure ethane. This confirms the p-type character of all the samples in the presence of ethane. Finally, the air sequence was repeated for confirming the reversibility of the phenomena. Except for Nb–NiO, we noted, as expected, a more important decrease of the electrical conductivity of the M–NiO samples in pure ethane than in an ethane–air mixture. This state corresponds to the maximum reduction of the solid in the presence of ethane. In the case of Nb–NiO, the maximum reduction of the solid seemed also to be reached in the ethane–air mixture. Nb–NiO was by far the most active catalyst in the ethane ODH reaction, as shown in Table 1. In addition, total conversion of oxygen was observed at 400 °C during the catalytic reaction.[25] Therefore, Nb–NiO exhibits the same reduction in conductivity in both ethane and ethane–air mixture as oxygen is probably depleted also in the latter case.

The observed decrease of the electrical conductivity of the M–NiO catalysts in the presence of ethane suggests that ethane is transformed by consuming the positive holes existing in the p-type oxide catalyst. It can thus be proposed that the initial activation step of ethane is a C–H bond cleavage *via* the attack by a positive hole. If one considers that from the chemical point of view, a positive hole corresponds to an electron vacancy in the valence band of lattice $O_O^{\times}$ anions, *i.e.* the ''chemical site'' of a positive hole corresponds in fact to a lattice $O_O^{\bullet}$ anion,[21] according to the reaction:

$$O_O^{\times} + h^{\bullet} \rightleftarrows O_O^{\bullet} \quad (16)$$

the activation of ethane over M–NiO catalysts can be written:

$$C_2H_6 + O_O^{\bullet} \rightarrow C_2H_5^{\bullet} + (HO^-)^{\bullet} \quad (17)$$

Water elimination generates oxygen vacancies, according to the reaction:

$$2(HO^-)^{\bullet} \rightleftarrows H_2O_{(g)} + O_O^{\times} + V_O^{\bullet\bullet} \quad (18)$$

These vacancies must be filled in by gaseous oxygen in order to reoxidize the solid:

$$\tfrac{1}{2}O_{2(g)} + V_O^{\bullet\bullet} \rightarrow O_O^{\times} + 2h^{\bullet} \quad (19)$$

This is in line with the observed ''breathing'' redox behavior of the solids under different gaseous atmospheres and suggests that the overall reaction mechanism of M–NiO catalysts can be assimilated to a Mars–van Krevelen type mechanism[30] involving surface lattice O^- species (*i.e.* $O_O^{\bullet}$).

It is interesting to note that the absolute conductivity level of the oxides in the reaction mixture decreases with increasing valence of the dopants, as follows: Li–NiO > NiO > Mg–NiO > Al–NiO > Ga–NiO > Ti–NiO > Nb–NiO. This means that the concentration of the charge carriers, *i.e.* positive holes, decreases following the same order. If we take into consideration that the ''chemical site'' of a positive hole is an O^- species according to eqn (16), and that these species, quite active for alkane oxidation, at high concentration might promote ethane combustion rather than oxidative dehydrogenation,[31] we can explain why the ODH selectivity increases with increasing

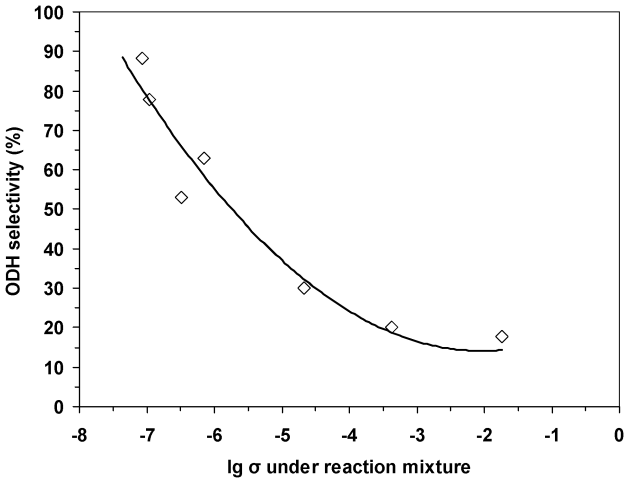

Fig. 7 Variation of the ethylene selectivity at isoconversion at 400 °C as a function of the electrical conductivity in the reaction mixture for NiO and M–NiO catalysts, with M = Li, Mg, Al, Ga, Ti and Nb (σ in ohm^{-1} cm^{-1}).

valence of the dopants following the order: Li–NiO < NiO < Mg–NiO < Al–NiO < Ga–NiO < Ti–NiO < Nb–NiO. This inverse correlation between the ODH selectivity and the conductivity level of the oxides under the reaction conditions is plotted in Fig. 7. However, it can be observed that the correlation is not linear suggesting that the electrical conductivity is not the only factor influencing the ODH selectivity. These results are in perfect agreement with findings from TPD–O_2 experiments over the same catalysts reported in ref. 25. According to these measurements, the sample is heated under temperature programmed conditions in helium flow. It was found that oxygen, corresponding to non-stoichiometric O^- species, desorbs at high temperature. Characterization of the M–NiO catalysts showed that the dissolution of lower than nickel valence cations (Li^+) increases the non-stoichiometric oxygen in NiO, while the higher valence cations (Al^{3+}, Ga^{3+}, Ti^{4+} and Nb^{5+}) reduce the positive hole concentration and consequently the electrophilic oxygen radicals of the NiO acceptor.[25] The amount of this oxygen determined by TPD–O_2 was again inversely correlated with ethylene selectivity, highlighting and confirming the importance of these species in the ethane ODH reaction.

Let us consider the difference, in terms of $\lg\sigma$, between the value of the electrical conductivity under air, which corresponds to a fully oxidized solid, and the value of the electrical conductivity in the reaction mixture (ethane–air mixture), denoted $\Delta(\lg\sigma)$. The electrical conductivity decreased when the reaction mixture passed over the sample, this means that the solid was reduced and the $\Delta(\lg\sigma)$ value can be considered a measure of the number of lattice oxygen species removed from the solid in the reaction mixture compared to that under air. This corresponds to the real degree of reduction of the solid during catalysis and it increases with increasing valence of the dopants in the following order: Li–NiO < NiO < Mg–NiO < Al–NiO < Ga–NiO < Ti–NiO < Nb–NiO. Except for the Ti–NiO sample, a correlation between the total oxygen atoms exchanged per gram of the catalyst in temperature-programmed $^{18}O_2$

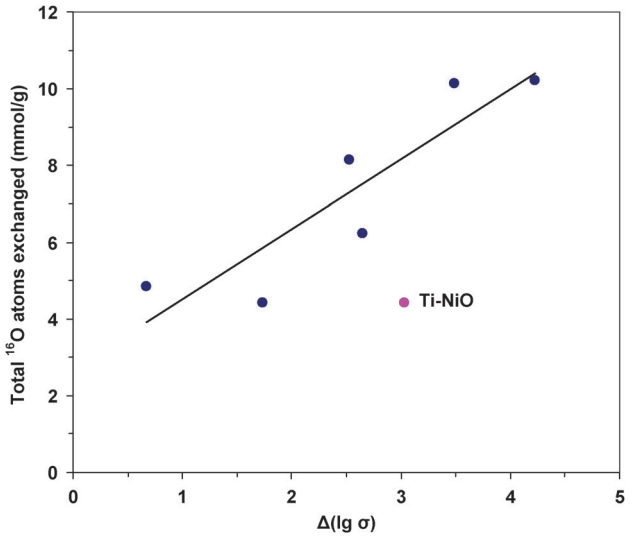

Fig. 8 Variation of the total oxygen atoms exchanged in the temperature-programmed $^{18}O_2$ isotope exchange experiments (data from ref. 25) as a function of the number of lattice oxygen species removed from the solid in the reaction mixture expressed as $\Delta(\lg \sigma)$.

isotopic oxygen experiments (data from ref. 25) and the number of lattice oxygen species removed from the solid in the reaction mixture compared to that under air expressed as $\Delta(\lg \sigma)$ was observed (Fig. 8). This suggests that the exchanged O atoms and the surface oxygen species removed in the presence of the reaction mixture are the same. Moreover, except for the Ti–NiO sample, a linear correlation between the apparent activation energy of the isotopic oxygen exchange reaction (E_a) for the M–NiO mixed oxides taken from ref. 25 and their activation energy of conduction (E_c) was also observed (Fig. 9). This suggests that the same oxygen species are involved in both the oxygen exchange and the conduction mechanism, confirming

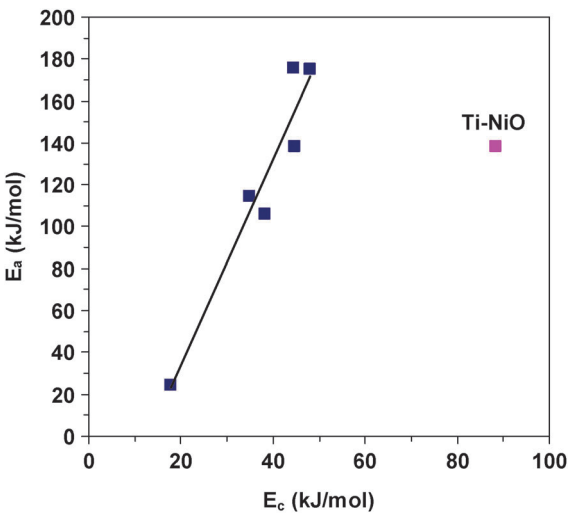

Fig. 9 Variation of the apparent activation energy of the isotopic oxygen exchange reaction (E_a) (data from ref. 25) as a function of the activation energy of conduction (E_c) for the NiO and M–NiO catalysts, with M = Li, Mg, Al, Ga, Ti and Nb.

that the positive holes are associated with the oxygen species in the solid. The behavior of the Ti–NiO sample can be explained by an electron transfer from TiO_2 to NiO, as discussed in Section 3.2.

Finally, we note that the catalytic activity expressed as the intrinsic rate of ethane consumption which decreased in the following order: Li–NiO > Mg–NiO > NiO > Nb–NiO > Ti–NiO > Ga–NiO > Al–NiO, roughly follows, except for Ti–NiO, the electrical conductivity of the solid under air. This means that the higher the concentration of charge carriers, *i.e.* positive holes, the higher the catalytic affinity for ethane. In other words, as expected, the higher the concentration of available O^- species, the higher the rate of ethane transformation. The presence of a TiO_2 phase in the Ti–NiO catalyst could explain its different behavior.

4. Conclusion

The electrical conductivity measurements showed that all the M-doped NiO samples, with M = Li, Mg, Al, Ga, Ti, Nb, were p-type semiconductors both under air and in the ethane–air reaction mixture at 400 °C. Except for Nb–NiO, their electrical conductivity decreased and the activation energy of conduction increased with increasing valence of doping cations. The different behavior of Nb–NiO was explained by a reduction of the niobium doping cation valence. All the catalysts are partially reduced during catalysis. The ODH selectivity was higher as the p-type semiconductivity in the reaction mixture was lower. On the other hand, the catalytic activity roughly followed the p-type semiconductivity of the catalysts under air. These correlations with the catalytic results indicate that O^- species are the active sites for ethane activation, however conversion to the targeted product, ethylene, occurs only when their concentration is low and the attack to the activated ethane is milder. *In situ* changes in the electrical conductivity under different gaseous atmospheres provide clear and direct evidence for a redox mechanism with consumption of surface lattice oxygen. It can be assimilated to a Mars–van Krevelen type mechanism involving surface lattice O^- species.

Acknowledgements

Ionel Popescu express his gratitude to the management staff of the University of Bucharest, especially to the Vice Rector Prof. Emil Barna, for the financial support.

References

1 J. M. Herrmann, *Catal. Today*, 2006, **112**, 73–77.
2 J. M. Herrmann, in *Catalyst Characterization, Physical Techniques for Solid Materials*, ed. B. Imelik and J. C. Védrine, Plenum Press, New York, 1994, ch. 20.
3 L. M. Madeira, J. M. Herrmann, J. Disdier, M. F. Portela and F. G. Freire, *Appl. Catal., A*, 2002, **235**, 1–10.
4 I. C. Marcu, J. M. M. Millet and J. M. Herrmann, *Catal. Lett.*, 2002, **78**, 273–279.

5 J. M. Herrmann, F. Villain and L. G. Appel, *Appl. Catal., A*, 2003, **240**, 177–182.
6 J. M. M. Millet, I. C. Marcu and J. M. Herrmann, *J. Mol. Catal. A: Chem.*, 2005, **226**, 111–117.
7 O. V. Safonova, B. Deniau and J. M. M. Millet, *J. Phys. Chem. B*, 2006, **110**, 23962–23967.
8 M. Caldararu, M. Scurtu, C. Hornoiu, C. Munteanu, T. Blasco and J. M. López Nieto, *Catal. Today*, 2010, **155**, 311–318.
9 G. Mitran, A. Urdă, I. Săndulescu and I. C. Marcu, *React. Kinet., Mech. Catal.*, 2010, **99**, 135–142.
10 I. Popescu, I. Săndulescu, Á. Rédey and I. C. Marcu, *Catal. Lett.*, 2011, **141**, 445–451.
11 A. Simon and E. V. Kondratenko, *Appl. Catal., A*, 2011, **392**, 199–207.
12 Y. Maeda, Y. Iizuka and M. Kohyama, *J. Am. Chem. Soc.*, 2013, **135**, 906–909.
13 A. Vasile, V. Bratan, C. Hornoiu, M. Caldararu, N. I. Ionescu, T. Yuzhakova and Á. Rédey, *Appl. Catal., B*, 2013, **140–141**, 25–31.
14 R. Dziembaj, M. Molenda, M. M. Zaitz, L. Chmielarz and K. Furczoń, *Solid State Ionics*, 2013, **251**, 18–22.
15 G. H. Yi, T. Hayakawa, A. G. Andersen, K. Suzuki, S. Hamakawa, A. P. E. York, M. Shimizu and K. Takehira, *Catal. Lett.*, 1996, **38**, 189–195.
16 Q. J. Ge, B. Zhaorigetu, C. Y. Yu, W. Z. Li and H. Y. Xu, *Catal. Lett.*, 2000, **68**, 59–62.
17 B. Zhaorigetu, W. Li, H. Xu and R. Kieffer, *Catal. Lett.*, 2004, **94**, 125–129.
18 P. Viparelli, P. Ciambelli, J. C. Volta and J. M. Herrmann, *Appl. Catal., A*, 1999, **182**, 165–173.
19 E. V. Kondratenko and M. Baerns, *Appl. Catal., A*, 2001, **222**, 133–143.
20 L. M. Madeira, J. M. Herrmann, F. G. Freire, M. F. Portela and F. J. Maldonado, *Appl. Catal., A*, 1997, **158**, 243–256.
21 J. M. Herrmann, P. Vernoux, K. E. Béré and M. Abon, *J. Catal.*, 1997, **167**, 106–117.
22 A. M. D. Farias, W. Gonzalez, P. G. Pries, J. G. Eon, J. M. Herrmann, M. Aouine, S. Loridant and J. C. Volta, *J. Catal.*, 2002, **208**, 238–246.
23 C. Yu, W. Li, W. Feng, A. Qi and Y. Chen, *Stud. Surf. Sci. Catal.*, 1993, **75**, 1119–1130.
24 V. Soenen, J. M. Herrmann and J. C. Volta, *J. Catal.*, 1996, **159**, 410–417.
25 E. Heracleous and A. A. Lemonidou, *J. Catal.*, 2010, **270**, 67–75.
26 E. Heracleous and A. A. Lemonidou, *J. Catal.*, 2006, **237**, 162–174.
27 G. A. El-Shobaky and N. Sh. Petro, *Surf. Technol.*, 1979, **9**, 415–426.
28 J. M. Herrmann, E. Ramaroson, J. F. Tempere and M. F. Guilleux, *Appl. Catal.*, 1989, **53**, 117–134.
29 E. W. McFarland and H. Metiu, *Chem. Rev.*, 2013, **113**, 4391–4427.
30 S. Mars and N. van Krevelen, *Chem. Eng. Sci.*, 1954, **9**(special suppl), 41–57.
31 Z. Skoufa, E. Heracleous and A. A. Lemonidou, *Catal. Today*, 2012, **192**, 169–176.

